Crack Detection in A Cantilever Beam Using Correlation Model and Machine Learning Approach

Vikas KHALKAR
Faculty, Gharda Institute of Technology, Lavel, India,
e-mail: vikas_khalkar@rediffmail.com

Pratik OAK
Faculty, Gharda Institute of Technology, Lavel, India,
e-mail: pvoak@git-india.edu.in

A MOSHI
Faculty, National Engineering College, Kovilpatti, India,
e-mail: moshibeo2010@gmail.com

Pon HARIHARASAKHTISUDHAN
Faculty, Sri Krishna College of Technology, Kovaipudur, India,
e-mail: harimeed2012@gmail.com

Lalitkumar JUGULKAR
Faculty, Rajarambapu Institute of Technology, Islampur, Sangli, India,
e-mail: lalitkumar.jugulkar@ritindia.edu

Raman BANE
Faculty, Gharda Institute of Technology, Lavel, India,
e-mail: rrbane@git-india.edu.in

Abstract: - Crack in a structural member alters local stiffness that affects the dynamic response, such as natural frequency and mode shapes. The purpose of structural health monitoring is to diagnose and predict structural health. In this paper, a correlation model is developed to detect crack parameters, i.e., crack location and crack depth, in the beam. To evaluate the authenticity of the developed correlation model, the Artificial Intelligence-based approach is used to predict the crack parameters. Twenty-three Artificial Intelligence algorithms were used to predict the locations and depths of the crack in a cantilever beam. The developed correlation model used the first two normalized natural frequencies to predict the crack parameters. On the other hand, the first three normalized natural frequencies were used to input the machine learning models to predict the crack parameters. In this research study, V-shaped and U-shaped open edges cracks were considered on the cantilever beam. FEA software, ANSYS, is used to do the modal vibration analysis of various cracked cases of beams. The data set of V-shaped and a U-shaped cracked case obtained from finite element analysis (FEA) were used to develop the correlation model and machine learning models. The results for crack locations and crack depth obtained from the correlation model and machine learning models agree with the actual results. In the future, the proposed correlation model of crack detection can be used to detect cracks in more complicated structures.

Keywords: - Correlation model, ANN, Machine learning, Natural frequency, FEA and Crack location.

1. INTRODUCTION

Beams are used in various structural applications in the automotive, civil, and aerospace industries. The presence of crack affects the structure's stiffness and affects the mechanical response of the whole structure to a more considerable extent. Due to these changes, there is a reduction in modal frequencies and mode shapes. Therefore, it is feasible to anticipate the crack characteristics by determining changes in the vibration parameters [1].

A fault diagnosis method based on genetic algorithms (GAs), and a model of damaged (cracked) structure is proposed. For modeling the cracked-beam structure an analytical model of a cracked cantilever beam is utilized, and natural frequencies were

obtained using numerical methods. This method utilized genetic algorithms to monitor the possible changes in the natural frequencies of the structure. The identification of the crack location and depth in the cantilever beam is formulated as an optimization problem, and binary and continuous genetic algorithms (BGA, CGA) are used to find the optimal location and depth by minimizing the cost function which is based on the difference of measured and calculated natural frequencies. Khatir et al. [2] presents a methodology for nondestructive detection, localization, and quantification of various damages in simple and continuous beams, as well as a more sophisticated structure, the two-dimensional frame structure.

The Firefly Algorithm and Genetic Algorithm are employed as optimization methods, while the Coordinate Modal Assurance Criterion is used as an objective function in the suggested methodology. The findings suggest that the proposed combination of the Coordinate Modal Assurance Criterion and the Firefly Algorithm or Genetic Algorithm can be utilized to quickly discover various local structural faults in complex structures. Visual inspection of cracks and damages is unsuitable and not worth considering in most cases; thus, non-destructive testing (NDT) methods like thermography, ultrasonic testing, X-ray diffraction, etc., are used to predict damage in the structures. However, these methods require time and expenses. So the other possible methods are motivated to be developed [3]. In this analogy, the use of mathematical methods, vibration-based methods, and soft-computing techniques such as artificial neural networks (a subfield of artificial intelligence) are promising and favorable.

Nasiri et. Al [4] presented a review paper utilizing Artificial Intelligence (AI) methods for mechanical fault detection. They discussed the applications of Bayesian networks, GA (genetic algorithms), fuzzy logic, case-based reasoning, and ANN, i.e., artificial neural networks. Sutar et al. [3] investigated transverse crack in cantilever beam by proposing a neural network-based controller. Crack stiffness to beam elemental stiffness matrix was used to obtain a homogenous linear elastic beam finite element by Teidj et al. [5] and used the measurement of the changes in the beam frequencies and observed their variations to detect the crack defect characteristics.

Thatoi et al. [6] described the Cascade Forward Back Propagation (CFBP) network to detect cracks in structural beams with the idea of changes in the natural frequencies and their measurements. Pan et al. [7] developed a two-stage approach combining of artificial neural network (ANN) and genetic algorithm (GA) to identify crack characteristics. Orhan et al. [8] introduced the new crack model (combination of V-shaped and Rectangular shaped crack) with the known V-shaped cracked model in order to investigate the effect of geometry change on the natural frequencies and mode shapes under free vibration loading. The result of this study reveals that composite structures are less sensitive for the geometry change as long as vibration characteristics are concerned. Gillich et al. [17] proposed two machine learning methods, random forest (RF) and the artificial neural network (ANN), as searching tools in this paper. Their databases contain damage scenarios for a prismatic cantilever beam with one crack and ideal and non-ideal boundary conditions.

The crack assessment was made in two steps. First, a coarse damage location was found from the networks trained for scenarios comprising the whole beam. Afterward, the assessment was made involving a particular network trained for the segment of the beam on which the crack was previously found. They used the two machine learning methods to estimate the crack location and severity with high accuracy for both simulation and laboratory experiments.

Regarding the location of the crack, which was the main goal of the practitioners, the errors were less than 0.6%. Based on these achievements, they concluded that the damage assessment we proposed, in conjunction with the machine learning methods, is robust and reliable. In this paper, Tufisi et al. [18] proposed a model for detecting transverse cracks in simply supported beams, which can be part of more complex structural systems. The relative frequency shifts of the structure are considered a basis for damage identification.

An original method developed by the authors is employed to evaluate the required modal parameters. A multi-stage optimization approach based on the rigidity loss suffered by the affected structure is employed to recognize the locations of potential cracks accurately. The outcome presented in this research shows the computational ability of the proposed model to indicate the presence and location of damages in the beam-like structures. In this study, Tufisi et al. [19] present a method (DS-SHC) used for estimating the DS for closed and open transverse cracks in beam-like structures using the intact and damaged beam deflections under its weight and a Stochastic Hill Climbing (SHC) algorithm. After describing the procedure of applying DS-SHC, we calculate for a prismatic cantilever beam the severities for different crack types and depths. The results are tested by comparing the DS obtained with DS-SHC with those acquired from dynamic tests made using professional simulation software.

We obtained a good fit between the severities determined in these two ways. Subsequently, they performed laboratory experiments and found that the

severities obtained with the DS-SHC method can accurately predict the frequency changes due to the crack. Hence, these severities are a valuable tool for damage detection.

In this paper, Tufisi et al. [20] proposed an analytical approach for generating the data needed to train a Random Forest model (RF) that will perform the SHM task to detect, locate, and assess the severity of transverse cracks in beam-like structures.

Using an original method, they calculated the relative frequency shifts (RFS) for different damage scenarios and used the generated data to train the RF model. Subsequently, the RF model is validated using data obtained from FEM simulations using different mesh sizes for different damage scenarios on steel beams.

The results indicate that the RF model can detect the presence of the defect and find the position and depth of the transverse cracks very precisely if the crack is located in the area where the beam achieves the maximum bending moment. By correctly categorizing accelerometer data, deep learning algorithms achieve the objective [21] of evaluating the condition of beams in a non-invasive manner. While an essential indicator, the high probabilistic accuracy attained on the validation set is typically insufficient in most practical circumstances.

When damage occurs, the accurate prognosis must also be comprehensible to humans, considering the factors that led to that specific outcome. It will increase confidence and the chance of rectifying functioning conditions in the future. We use the LIME and SHAP algorithms to correlate model-neutral global and local explanations to create an interpretable model. We offer a compound stability-fit compensation index due to the potential instability of the local explanations.

The action of fatigue load on structures results in single-sided open-edged cracks. Stress corroded turbine blades cause localized loss of the material in them. After removing the localized material from the blade, the damage location can be mapped into U-shaped or V-shaped open-edged cracks. As a result, this research study has considered two types of open-edged crack on the cantilever beam.

The research paper's analysis is separated into two parts. The natural frequencies for various V-shaped and U-shaped open-edged cracked cases were determined using the numerical method in the first half.

Furthermore, in the second half, a developed correlation model and machine learning approach were employed to cracked beam to detect the crack parameters in the cantilever beam.

2. INVERSE METHOD OF CRACK DETECTION WITH CORRELATION MODEL

This research study proposes a correlation model between the normalized natural frequencies and normalized crack parameters, i.e., crack location and crack depth, as a forward approach. It is given in Equation (1).

$$Y = f\left(\frac{L_1}{L}, \frac{a}{H}\right) \tag{1}$$

Y is the ratio between the natural frequency of the cracked beam and the natural frequency of the un-cracked beam.

L_1/L is the ratio of the distance of the crack from the cantilevered end to the length of the beam.

a/H is the ratio of crack depth to the depth of the beam.

$$f\left(\frac{L_1}{L}, \frac{a}{H}\right) - Y = 0 \tag{2}$$

Then, inverse method using correlation model is proposed to detect the location and depth of the crack in a cantilever beam.

3. CORRELATION MODEL

The natural frequencies of the cracked beam were normalized with that of the intact beam. Y_1 and Y_2 are the normalized natural frequencies in the first and second modes, respectively. They were plotted against the dimensionless crack parameters, i.e., crack location and crack depth. The first and second natural frequencies were used to obtain the correlation model for the curve fitting. Only two equations were required to find two unknown crack parameters, i.e., crack location and depth. Based on the non-linear relationship between crack parameters and frequency ratios, non-linear polynomial curve fitting was used to get two equations for two natural frequency ratios at the first and second modes. Equations 3 and 4 were developed using the data set of V-shaped cracked cases.

Similarly, Equations (5) and (6) were developed using the data set of U-shaped cracked cases. The data set of V-shaped and U-shaped cracked cases are presented in Table 1. Correlation models for the natural frequencies ratio at the first and second modes for V-shaped cracked cases were developed, and they are given in Equation (3) and Equation (4), respectively. Similarly, the correlation models for the natural frequencies ratio at the first and second modes

for U-shaped cracked cases were developed. They are given in Equation (5) and Equation (6), respectively.

$$1.03190 - \left(0.24618 * \left(\frac{L_1}{L}\right)\right) - \left(0.10796 * \left(\frac{a}{H}\right)\right) + \left(0.60948 * \left(\frac{L_1}{L}\right) * \left(\frac{a}{H}\right)\right) + \left(0.46021 * \left(\frac{L_1}{L}\right)^2\right) - \left(0.54735 * \left(\frac{a}{H}\right)^2\right) - \left(0.90726 * \left(\frac{L_1}{L}\right)^2 * \left(\frac{a}{H}\right)\right) + \left(1.52640 * \left(\frac{L_1}{L}\right) * \left(\frac{a}{H}\right)^2\right) - (0.21756 * \left(\frac{L_1}{L}\right)^3) - \left(0.63026 * \left(\frac{a}{H}\right)^3\right) - Y_1 = 0 \quad (3)$$

$$0.82733 + \left(1.11904 * \left(\frac{L_1}{L}\right)\right) + \left(0.47147 * \left(\frac{a}{H}\right)\right) - \left(3.13757 * \left(\frac{L_1}{L}\right) * \left(\frac{a}{H}\right)\right) - \left(1.70394 * \left(\frac{L_1}{L}\right)^2\right) + \left(0.40455 * \left(\frac{a}{H}\right)^2\right) + \left(3.09003 * \left(\frac{L_1}{L}\right)^2 * \left(\frac{a}{H}\right)\right) - \left(0.34222 * \left(\frac{L_1}{L}\right) * \left(\frac{a}{H}\right)^2\right) + (0.70575 * \left(\frac{L_1}{L}\right)^3) - \left(0.53943 * \left(\frac{a}{H}\right)^3\right) - Y_2 = 0 \quad (4)$$

$$1.03189 - \left(0.26371 * \left(\frac{L_1}{L}\right)\right) - \left(0.11329 * \left(\frac{a}{H}\right)\right) + \left(0.56253 * \left(\frac{L_1}{L}\right) * \left(\frac{a}{H}\right)\right) + \left(0.53075 * \left(\frac{L_1}{L}\right)^2\right) - \left(0.55074 * \left(\frac{a}{H}\right)^2\right) - \left(0.86077 * \left(\frac{L_1}{L}\right)^2 * \left(\frac{a}{H}\right)\right) + \left(1.59538 * \left(\frac{L_1}{L}\right) * \left(\frac{a}{H}\right)^2\right) - (0.27456 * \left(\frac{L_1}{L}\right)^3) - \left(0.69112 * \left(\frac{a}{H}\right)^3\right) - Y_1 = 0 \quad (5)$$

$$0.81314 + \left(1.22783 * \left(\frac{L_1}{L}\right)\right) + \left(0.49187 * \left(\frac{a}{H}\right)\right) - \left(3.32663 * \left(\frac{L_1}{L}\right) * \left(\frac{a}{H}\right)\right) - \left(1.90931 * \left(\frac{L_1}{L}\right)^2\right) + \left(0.43864 * \left(\frac{a}{H}\right)^2\right) + \left(3.29483 * \left(\frac{L_1}{L}\right)^2 * \left(\frac{a}{H}\right)\right) - \left(0.39802 * \left(\frac{L_1}{L}\right) * \left(\frac{a}{H}\right)^2\right) + (0.81597 * \left(\frac{L_1}{L}\right)^3) - \left(0.56162 * \left(\frac{a}{H}\right)^3\right) - Y_2 = 0 \quad (6)$$

To determine the locations and depths of V-shaped cracks in a cantilever beam, Equation (3) and Equation (4) were used. Similarly, Equation (5) and Equation (6) were used to determine the locations and depths of U-shaped cracks in a cantilever beam. The third order correlation models presented in equations (3), (4), (5) and (6) were generated by performing regression analysis with the aid of Design Expert software.

The reliability of the correlation models is generally determined by the R-squared values. The R-squared value nearer to '1' represents the good fit of the data on the generated correlation models. In the present work, the R-squared values of the generated correlation models presented in equations (3), (4), (5) and (6) were found to be 0.9943, 0.8890, 0.9939 and 0.8914 respectively. As the R-squared values of all the generated correlation models are nearer to '1', the models are ensured to be reliable.

To predict the crack depth and crack locations in a V-shaped cracked beam, the first and second normalized frequencies were used and were substituted in Equation (3) and Equation (4), respectively. Afterward, Equations (3) and Equation (4) were solved simultaneously using Microsoft Excel to predict the locations and depth of V-shaped cracks in a cantilever beam.

Similarly, Equations (5) and Equation (6) were solved simultaneously using Microsoft Excel to predict the locations and depths of U-shaped cracks in a cantilever beam.

4. SIMULATED CRACK CONFIGURATIONS

Geometric properties: The cross-sectional area and length of the beam are 0.02 × 0.02 m^2 and 0.32 m, respectively.

Material properties: Young's modulus (E) = 2.104 x 10^{11} N/m^2 , Mass density (ρ) = 7820 kg/m^3 , Mass (M) = 1.00096 kg.

In this study, a total of 160 cracked specimens of steel materials were considered to investigate the effect of different kinds of cracks on the natural frequencies of a cantilever beam. The width of the crack (along the longitudinal direction) is chosen as 0.5 mm. Two separate cases were considered, i.e., case 1 and case 2.

Case 1: 80 specimens of V-shaped cracked cases were considered in this case. This case was subdivided into five sub-cases. In the first sub-case, 16 specimens were considered. 50 mm crack location was chosen for the crack, and at this location, crack depth was varied from 1 mm to 16 mm by an interval of 1 mm.

The second, third, fourth, and fifth sub cases were similar to that of the first sub-case; the only difference was that instead of 50 mm crack location; 100 mm, 150 mm, 200 mm, and 250 mm cracks locations were chosen for the second, third, fourth and fifth sub-cases respectively.

Case 2: Case 2 was like case 1; the only difference was that instead of V-shaped crack geometries, U-shaped crack geometries were considered on the specimens.

The one case of V-shaped and U-shaped cracked cases are shown in Figure 1 and Figure 2 respectively.

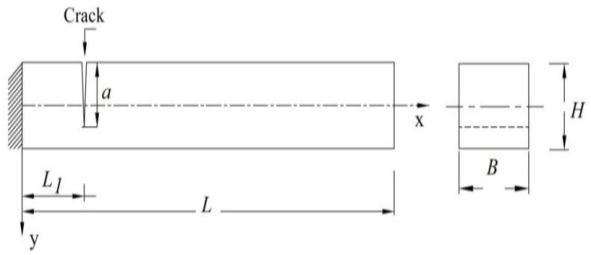

Figure 1. Cracked cantilever beam with V-shaped crack.

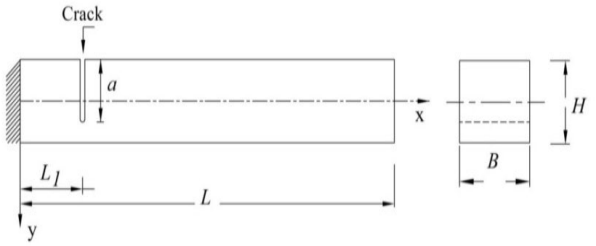

Figure 2. Cracked cantilever beam with U-shaped crack.

5. FINITE ELEMENT MODELING AND ANALYSIS

ANSYS finite element program [9] was used to determine the natural frequency of cracked cantilevered beams. For this purpose, a rectangular zone of the required geometric properties was created, and then this zone was extruded to obtain the model in three dimensions. A small area of dimensional requirements was created and extruded to represent the crack in the primary model. After that subtract command was used for subtracting the small volume from the volume of the primary model [10, 11, 22 & 23]. Then a cracked three-dimensional solid model gets obtained. A Solid 186 (tetrahedral) element was used to mesh the cracked model of a cantilever beam. After meshing, the FEA model carried 6159 elements. Results of natural frequencies remained almost the same irrespective of the sizes of the elements (5 mm, 6 mm, and 7 mm) tried in the analysis. Furthermore, a 5 mm mesh size was finalized to mesh all the models. This element has some unique features, i.e., stress stiffening, large strain, and large deflection. Finite element boundary conditions were applied on the beam to constrain all degrees of freedom of the cantilevered end of the beam. The Block Lanczos eigenvalue solver was used to compute the natural frequencies of cracked beams. Mesh independent study was carried out to study the effect of mesh size on the natural frequency of cracked beams. Through mesh-independent study, it was found that natural frequency results were independent of the mesh size. Figures 3–5 illustrate a few natural frequency plots.

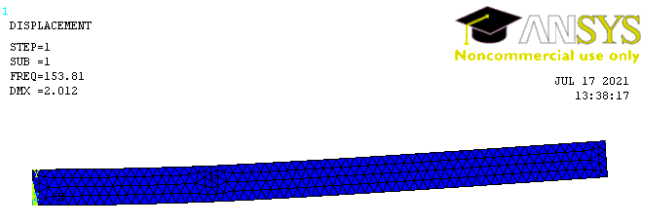

Figure 3. First natural frequency plot of V-shaped cracked case: Location ratio= 0.3125; depth ratio= 0.4.

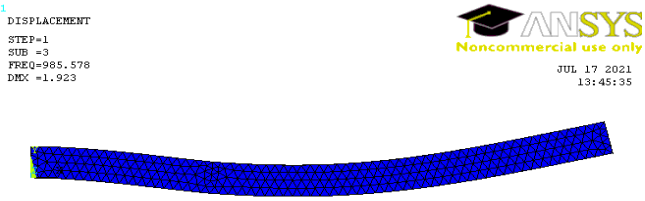

Figure 4. Second natural frequency plot of V-shaped cracked case: Location ratio= 0.3125; depth ratio= 0.4.

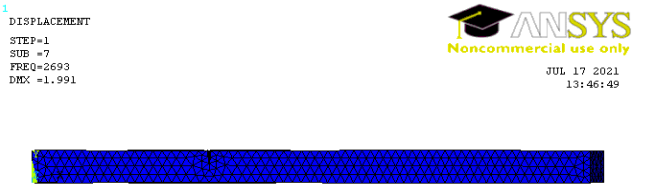

Figure 5. Third natural frequency plot of V-shaped cracked case: Location ratio= 0.3125; depth ratio= 0.4.

6. METHODLOGY

To predict the crack depth and crack locations in the beams, the input and output variables have normalized; hence, they are in the same range of 0 to 1.

The actual experimental results were compared with the simulation through machine learning-based classifiers. *Machine learning* is the self-prediction methodology that takes a few parameters as an input and known output responses. Based on these two input data, the algorithms generate a self-learning model. Various algorithms are suggested [15] in the state-of-art methods and they are used in most prediction related applications.

Decision Tree, Discriminant Analysis, Support Vector machines, Nearest Neighbor, Ensemble classifier, and Artificial Neural Network-based prediction are made in the proposed work. These classifier algorithms have their own trained model generation principles and few sub-algorithms. The discriminant analysis works on assuming different Gaussian distributions based on data generation. For linear discriminant analysis, each model class has the

same covariance matrix with varying mean values. In contrast, variations in both mean and covariance of each class are in the quadratic discriminant analysis (QDA). Predict classifies to minimize the expected classification cost. The SVM binary classification algorithm finds an optimal hyper-plane that separates the data into two classes. Depending on the homogeneity of the input parameters, the width of the hyper-plane varies. Prediction can be made for more accuracy [13-14] using linear or non-linear filters/kernels. A k-nearest neighbor classifier known as KNN is based on a distance metric. It has various distance metrics like cosine, cubic, Euclidean (weighted), etc. This classifier is considered one of the most straightforward prediction techniques.

Ensemble classifier uses a vote of different classifiers for class prediction. Five ensemble classifiers are most commonly used in state-of-art methodologies viz. Ensemble Boosted Trees, Ensemble Bagged Trees, Ensemble Subspace Discriminant, Ensemble Subspace KNN, and Ensemble RUS Boosted Trees.

The Decision Tree classifier predicts [12] on a hierarchy basis. It does not require any pre-requisite knowledge and is also considered as most straightforward prediction technique.

An artificial neural network (ANN) is a famous technique [15] that resembles the human brain guessing mechanism. It is the artificial intelligence (AI) base preferred for most complex problems. Feed forward ANN is the method we used in our proposed work. Performance Metrics Used for Analysis.

Confusion Matrix- The tabular representation of prediction performance and error factor is called as confusion matrix. It shows the performance as predicted class Vs true class.

AUC Curve- The graph showing [16] the model performance at all thresholds is called as ROC curve. It plots two parameters as true positive (TP) and false positive (FP). Area under the ROC curve is called as AUC. It is aggregate measure of performance and ranges between 0 (100% wrong) & 1 (100% correct).

7. RESULTS AND DISCUSSION

Numerical method was used to examine the natural frequencies of cracked cantilever beams with various crack depths, crack locations and crack geometries. Then the relationship between different cracked geometries and natural frequencies is investigated. The data tabulated in Table 1 are the neural network's training data for V-shaped and U-shaped cracked cases.

As explained in methodology, we made a comparative analysis of various classifiers as prediction algorithms. All classifiers are trained with a cross-validation factor 5. The standard Classifier learning app available in MATLAB 2018a had used for classification. Details of a parameter we used for each classifier are tabulated in Table 2. A comparison of performances of all the classifiers for accuracy is tabulated in Tables 3 and 4. The experimentation was carried out for both V-shaped and U-shaped cracked cases of a cantilever beam for crack parameters, i.e., crack location (L_1/L) and crack depth ratios (a/H). Classifiers outperformed for predicting the crack locations, i.e., L_1/L in beams. However, the accuracy of the same classifiers is poor for predicting the depth of the crack in beams, i.e., a/H. Quadratic discriminated analysis (QDA) had given the highest accuracy for predicting crack locations. It gave 94.3% accuracy for V-shaped cracked cases and 90.8% for U-shaped cracked cases. The confusion matrix and AUC curve represent better results given by this QDA. The Confusion Matrix of Quadratic Discriminated Analysis of U-shaped and V-shaped cracked cases is shown in Figure 6.

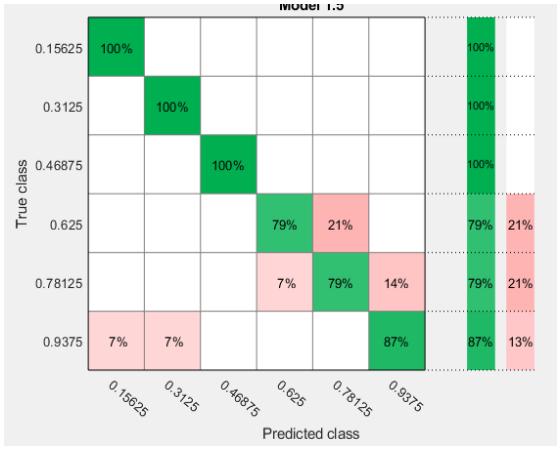

a) **U-shaped Confusion Matrix**

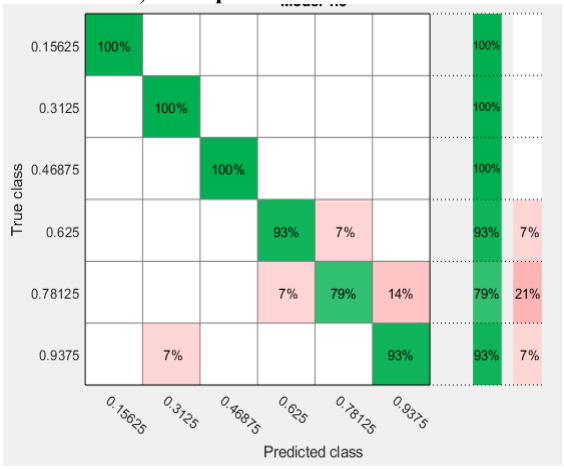

b) **V-shaped Confusion Matrix**

Figure 6. Confusion Matrix of Quadratic Discriminant Analysis (QDA)

AUC Curve of Quadratic Discriminated Analysis is shown in Figure 7. The graph shows the model performance at all thresholds is called as ROC curve.

However, the performance of ANN is best for predicting the crack parameters of defective beams amongst all 22 classifiers.

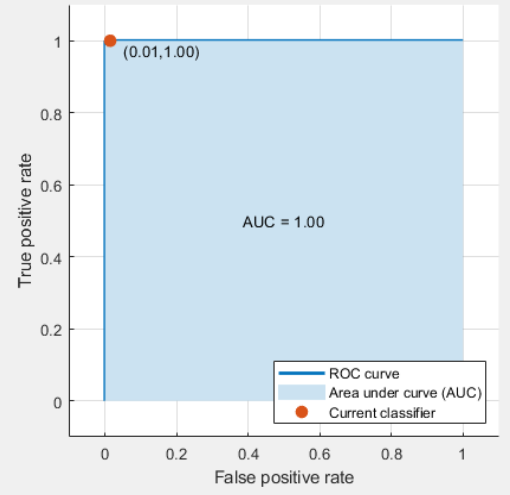

a) **U-shaped AUC Curve**

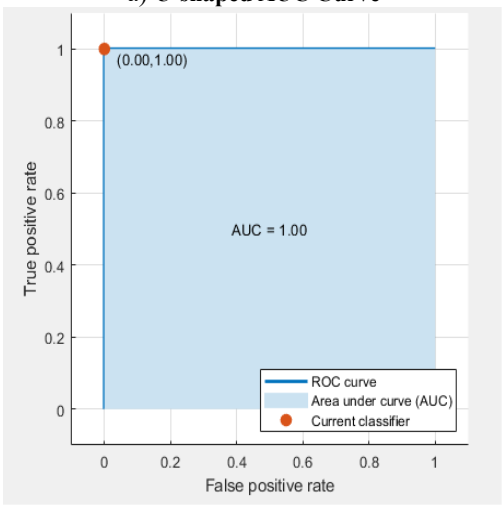

b) **V-shaped AUC Curve**

Figure 7. AUC Curve of Quadratic Discriminant Analysis (QDA)

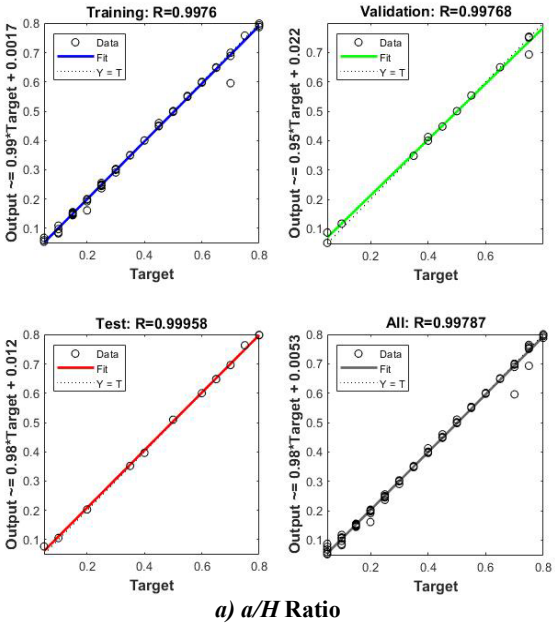

***a) a/H* Ratio**

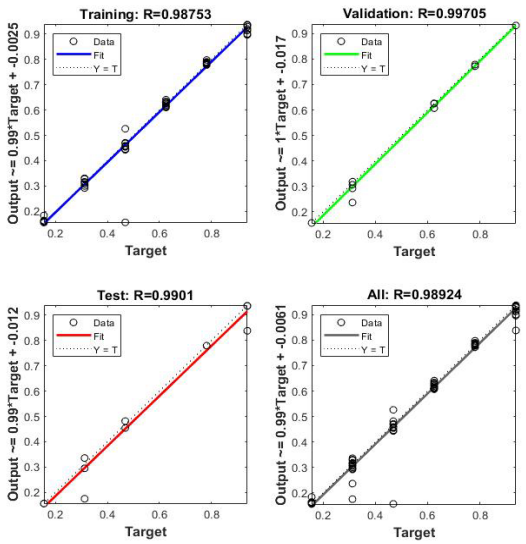

b) ***L*$_1$*/L* Ratio**

Figure 8. Performance of ANN for U-shaped cracked cases

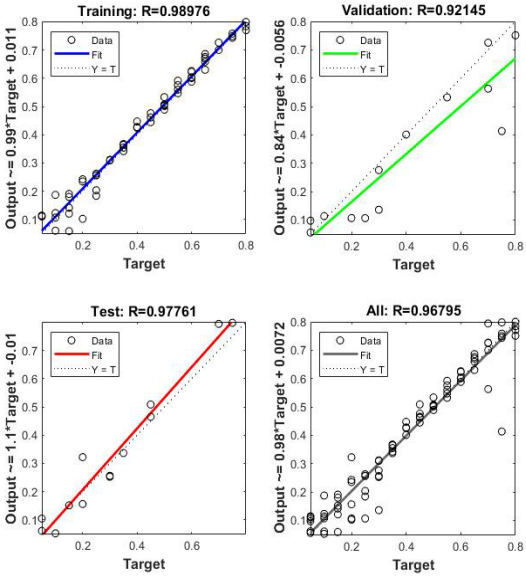

a) ***a/H* Ratio**

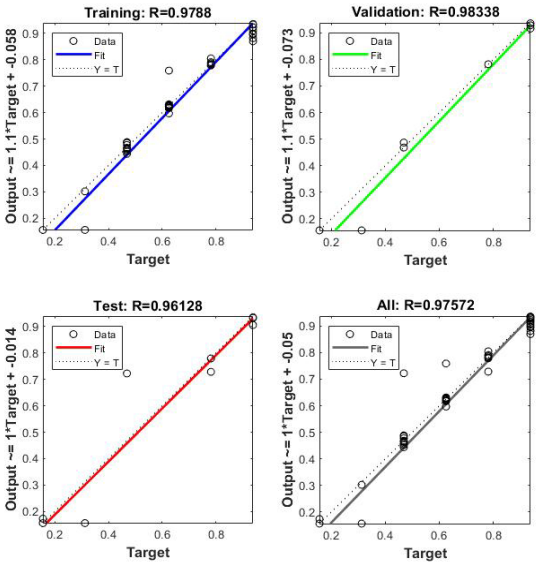

***b) L*$_1$*/L* Ratio**

Figure 9. Performance of ANN for V-shaped cracked cases.

The performance of ANN for both U-shaped and V-shaped cracked cases is shown in Figure 8 and 9 respectively.

The predicted crack depths (a/H) and crack locations (L_1/L) using ANN and correlation model for V-shaped and U-shaped cracked cases are presented in Table 5 and Table 6. From, Figure 10 and 11, it is clear that the correlation model and ANN model gives good prediction for the crack depths and crack locations. The predicted crack depths and crack locations are compared with the actual crack parameters for the same configurations. When comparing the findings of Table 5, it is evident that the ANN model performed well in predicting the crack depths and positions in U-shaped cracked cases. As a result, the ANN model can better predict the occurrence of U-shaped cracks than V-shaped cracks in beams for the same configurations.

Table 1. Training data of V-shaped and U-shaped cracked cases to the neural network.

Sr. No.			V-shaped cracked cases: Relative natural frequency			U-shaped cracked cases: Relative natural frequency		
	a/H	L_1/L	f_{r1}	f_{r2}	f_{r3}	f_{r1}	f_{r2}	f_{r3}
1	0.05	0.15625	0.998778	0.999901	1	0.998228	0.999802	0.999964
2	0.1	0.15625	0.994563	0.999405	0.999891	0.992852	0.999305	0.999854
3	0.15	0.15625	0.986987	0.998611	0.999709	0.984054	0.998313	0.999636
4	0.2	0.15625	0.976356	0.997519	0.999454	0.972141	0.997023	0.999308
5	0.25	0.15625	0.962488	0.99603	0.99909	0.956317	0.995335	0.998944
6	0.3	0.15625	0.944282	0.994145	0.998653	0.937256	0.993351	0.998434
7	0.35	0.15625	0.922959	0.991911	0.998107	0.91294	0.990919	0.997815
8	0.4	0.15625	0.894673	0.989063	0.997378	0.88563	0.98813	0.997087
9	0.45	0.15625	0.864919	0.986195	0.99665	0.853006	0.984934	0.996213
10	0.5	0.15625	0.828262	0.982662	0.995667	0.814944	0.981362	0.995157
11	0.55	0.15625	0.786229	0.978861	0.994502	0.770345	0.977332	0.993919
12	0.6	0.15625	0.74053	0.974911	0.993337	0.719941	0.973025	0.992499
13	0.65	0.15625	0.682001	0.970177	0.991625	0.660679	0.968331	0.990824
14	0.7	0.15625	0.621579	0.965661	0.989987	0.595045	0.963478	0.988822
15	0.75	0.15625	0.548192	0.96047	0.987766	0.520192	0.958347	0.986455
16	0.8	0.15625	0.467675	0.955468	0.985253	0.435282	0.953176	0.983542
17	0.05	0.3125	0.999389	0.999802	0.999782	0.999022	0.999702	0.999636
18	0.1	0.3125	0.997067	0.999008	0.998835	0.99609	0.998611	0.998471
19	0.15	0.3125	0.992852	0.99742	0.997196	0.991386	0.996923	0.99665
20	0.2	0.3125	0.986804	0.995137	0.994902	0.984665	0.994442	0.994247
21	0.25	0.3125	0.978983	0.992279	0.992208	0.97599	0.991266	0.991298
22	0.3	0.3125	0.969208	0.988656	0.992208	0.96487	0.987227	0.987766
23	0.35	0.3125	0.956806	0.98419	0.98529	0.950819	0.982205	0.983724
26	0.5	0.3125	0.897055	0.963517	0.970507	0.886486	0.960193	0.967994
27	0.55	0.3125	0.867058	0.953613	0.963662	0.854778	0.94997	0.96144
28	0.6	0.3125	0.831745	0.942646	0.956671	0.81641	0.93816	0.954231
29	0.65	0.3125	0.787573	0.929248	0.948915	0.767595	0.923948	0.945711
30	0.7	0.3125	0.735215	0.914738	0.940468	0.708822	0.908178	0.936353
31	0.75	0.3125	0.666606	0.89731	0.929872	0.638258	0.890939	0.925794
32	0.8	0.3125	0.582521	0.878186	0.918111	0.547733	0.871586	0.912759
33	0.05	0.46875	0.999695	0.999206	0.999964	0.999572	0.998809	0.999927
34	0.1	0.46875	0.998717	0.99603	0.999891	0.99835	0.994839	0.999854
35	0.15	0.46875	0.996945	0.990304	0.999782	0.996273	0.98816	0.999636
36	0.2	0.46875	0.994379	0.982235	0.999527	0.993341	0.979188	0.999417
37	0.25	0.46875	0.990836	0.971427	0.999272	0.989492	0.967586	0.99909
38	0.3	0.46875	0.986376	0.958347	0.998944	0.98436	0.952848	0.998689
39	0.35	0.46875	0.980389	0.941832	0.998507	0.978128	0.935937	0.998179
40	0.4	0.46875	0.972507	0.921338	0.997925	0.969697	0.914629	0.99756
41	0.45	0.46875	0.963099	0.89863	0.997306	0.959311	0.890185	0.996869
44	0.6	0.46875	0.916422	0.808347	0.994575	0.906525	0.79343	0.99381
45	0.65	0.46875	0.888624	0.767507	0.993264	0.875794	0.75137	0.992281
46	0.7	0.46875	0.855327	0.726786	0.991917	0.836083	0.707572	0.990606

Sr. No.	a/H	L_1/L	V-shaped cracked cases: Relative natural frequency			U-shaped cracked cases: Relative natural frequency		
			f_{r1}	f_{r2}	f_{r3}	f_{r1}	f_{r2}	f_{r3}
47	0.75	0.46875	0.804741	0.678444	0.990023	0.780242	0.659964	0.988494
48	0.8	0.46875	0.732832	0.62761	0.987766	0.702346	0.611195	0.985982
49	0.05	0.625	0.999878	0.999206	0.999745	0.999878	0.998908	0.999636
50	0.1	0.625	0.999633	0.996328	0.998835	0.999572	0.995236	0.998507
51	0.15	0.625	0.999145	0.991207	0.997342	0.998961	0.989162	0.996759
52	0.2	0.625	0.99835	0.983674	0.995157	0.998106	0.980717	0.994465
53	0.25	0.625	0.997312	0.973869	0.992609	0.996945	0.969889	0.991589
54	0.3	0.625	0.995907	0.960967	0.989331	0.995479	0.956123	0.988166
55	0.35	0.625	0.994257	0.946149	0.985909	0.993463	0.938845	0.984307
56	0.4	0.625	0.991813	0.925715	0.981576	0.990958	0.918162	0.979901
57	0.45	0.625	0.988697	0.901737	0.976733	0.987659	0.893321	0.974913
58	0.5	0.625	0.985093	0.875506	0.972036	0.983382	0.86318	0.969342
59	0.55	0.625	0.979778	0.841048	0.96581	0.977334	0.825715	0.963079
62	0.7	0.625	0.949108	0.699226	0.943417	0.941227	0.67369	0.939084
63	0.75	0.625	0.927114	0.634835	0.933513	0.915078	0.607037	0.928743
64	0.8	0.625	0.89009	0.560341	0.922335	0.872434	0.534845	0.917128
65	0.05	0.78125	1	0.999802	0.999745	1	0.999702	0.999563
66	0.1	0.78125	1	0.999008	0.998726	1	0.998611	0.998325
67	0.15	0.78125	0.999939	0.997519	0.997014	1	0.996923	0.996286
68	0.2	0.78125	0.999878	0.995435	0.994502	1	0.994541	0.993664
69	0.25	0.78125	0.999817	0.992447	0.991516	0.999878	0.991137	0.990424
70	0.3	0.78125	0.999633	0.988547	0.987802	0.999756	0.98687	0.986419
71	0.35	0.78125	0.99945	0.984021	0.983797	0.999572	0.981322	0.981867
72	0.4	0.78125	0.999084	0.976509	0.978335	0.999267	0.973809	0.976296
73	0.45	0.78125	0.998717	0.967954	0.9724	0.9989	0.964768	0.97007
74	0.5	0.78125	0.998228	0.957265	0.965955	0.99835	0.952044	0.963006
75	0.55	0.78125	0.997495	0.941653	0.957472	0.997556	0.935788	0.954632
76	0.6	0.78125	0.996579	0.923035	0.948988	0.996457	0.913319	0.945383
77	0.65	0.78125	0.995112	0.895276	0.938683	0.994868	0.881937	0.933877
80	0.8	0.78125	0.983504	0.720058	0.894334	0.980694	0.683932	0.886069
81	0.05	0.9375	1.000061	1.000099	1	1.000061	1.000099	1
82	0.1	0.9375	1.000122	1.000099	0.999964	1.000244	1.000198	1
83	0.15	0.9375	1.000183	1.000099	0.999964	1.000367	1.000198	0.999964
84	0.2	0.9375	1.000244	1.000099	0.999854	1.000428	1.000198	0.999891
85	0.25	0.9375	1.000305	1.000099	0.999782	1.000611	1.000298	0.999782
86	0.3	0.9375	1.000367	1.000099	0.999636	1.000733	1.000298	0.999636
87	0.35	0.9375	1.000428	1.000099	0.99949	1.000855	1.000298	0.999454
88	0.4	0.9375	1.000489	1	0.999235	1.000978	1.000298	0.999235
89	0.45	0.9375	1.00055	0.999901	0.99898	1.0011	1.000198	0.998944
90	0.5	0.9375	1.000611	0.999802	0.998616	1.001222	1.000099	0.998544
91	0.55	0.9375	1.000672	0.999603	0.998179	1.001344	0.999901	0.998107
92	0.6	0.9375	1.000733	0.999405	0.997706	1.001466	0.999603	0.997524
93	0.65	0.9375	1.000794	0.998908	0.996978	1.001588	0.999206	0.996723
94	0.7	0.9375	1.000794	0.998313	0.996213	1.001711	0.998511	0.995776
95	0.75	0.9375	1.000855	0.99742	0.995084	1.001833	0.99742	0.994465
96	0.8	0.9375	1.000855	0.995534	0.993592	1.001894	0.995137	0.992609

Table 2. Parameter Set in Classifier experimentation

Classifier	Variant	Maximum Number of Splits	Split Criteria	-
Decision Tree	Fine Tree	100	Gini's diversity index	
	Medium Tree	20		
	Coarse Tree	4		
Discriminant Analysis	Variant	Discriminant Type	Amount of Regularization	Fill Coefficients (Property flag)

Classifier	Variant	Maximum Number of Splits	Split Criteria	-
	Linear Discriminant Analysis (LDA)	Linear	0	Off
	Quadratic Discriminant Analysis (QDA)	Quadratic	1	Off
Support Vector Machine	Variant	Kernel Function	Polynomial Order	Mapping and Kernel Scale
	Linear SVM	Linear	-	One-Vs-One and Auto
	Quadratic SVM	Polynomial	2	One-Vs-One and Auto
	Cubic SVM	Polynomial	3	One-Vs-One and Auto
K-nearest neighbor classifier	Variant Cosine KNN	Distance Cosine	Exponent -	Distance Weight Equal
	Cubic KNN	Minkowski	3	Equal
	Weighted KNN	Euclidean	-	Squared Inverse
Ensemble Classifier	Variant	Method	Number of Learning Cycles	Learners
	Boosted Trees	Adaboost M1	30	Template
	Bagged Trees	Bag	30	Template
	Subspace Discriminant	Subspace	30	Discriminant
	Subspace KNN	Subspace	30	K NN
	RUSBoosted Trees	RUSBoost	30	Template
Artificial Neural Network	Variant	Number of Nodes per layer	Number of Epochs	Learning Rate
	Feed forward back propagation	Input- 3 Hidden- 8 Output -1	1000	0.1

Table 3. Comparison of various classifier performances for V-shaped cracked cases.

Sr. No.	Training Algorithm (K=5)		Accuracy (%)	Accuracy (%)
			L_1/L	a/H
1	Decision Tree Algorithm	Fine Tree	64.4	14.9
2		Medium Tree	64.4	14.9
3		Coarse Tree	48.3	10.3
4	Discriminant Analysis Algorithm	Linear Discriminant Analysis	58.6	14.9
5		Quadratic Discriminant Analysis	94.3	11.5
6	Support Vector Machines	Linear SVM	63.2	23
7		Quadratic SVM	66.7	17.2
8		Cubic SVM	80.5	23
9		Fine Gaussian SVM	69	18.4
10		Medium Gaussian SVM	63.2	26.4
11		Coarse Gaussian SVM	47.1	12.6
12	Nearest Neighbor Algorithm	Fine KNN	77	9.2
13		Medium KNN	56.3	9.2
14		Coarse KNN	18.4	5.7
15		Cosine KNN	64.4	11.6
16		Cubic KNN	62.1	10.3
17		Weighted KNN	77	10.3
18	Ensemble Classifier	Boosted Trees	18.4	13.8
19		Bagged Trees	78.2	16.1
20		Subspace Discriminant	56.3	12.6
21		Subspace KNN	54	23
22		RUSBoosted Trees	40.2	18.4
23	Artificial Neural Network	Feed Forward Back Propagation	99.977	100

Table 4. Comparison of various classifier performances for U-shaped cracked cases.

Sr. No.	Training Algorithm (K=5)		Accuracy (%)	Accuracy (%)
			L_1/L	a/H
1	Decision Tree Algorithm	Fine Tree	57.5	18.4
2		Medium Tree	57.5	18.4
3		Coarse Tree	47.1	9.2
4	Discriminant Analysis Algorithm	Linear Discriminant Analysis	64.4	13.8
5		Quadratic Discriminant Analysis	90.8	10.3
6	Support Vector Machines	Linear SVM	70.1	24.1
7		Quadratic SVM	71.3	24.1
8		Cubic SVM	82.8	17.2
9		Fine Gaussian SVM	69	20.7
10		Medium Gaussian SVM	66.7	27.6
11		Coarse Gaussian SVM	48.3	18.4
12	Nearest Neighbor Algorithm	Fine KNN	80.5	11.5
13		Medium KNN	66.7	9.2
14		Coarse KNN	18.4	5.7
15		Cosine KNN	66.7	9.2
16		Cubic KNN	66.7	10.3
17		Weighted KNN	78.2	11.5
18	Ensemble Classifier	Boosted Trees	18.4	18.4
19		Bagged Trees	80.5	17.2
20		Subspace Discriminant	59.8	13.8
21		Subspace KNN	49.4	17.2
22		RUSBoosted Trees	37.9	17.2
23	Artificial Neural Network	Feed Forward Back Propagation	99.1	99.95

Table 5. Comparison between Actual and predicted ANN outputs of V-shaped and U-shaped cracked cases.

Predicted ANN results for V-shaped cracked cases									
Sr. No.	**f_{r1}**	**f_{r2}**	**f_{r3}**	***a/H***	***a/H***	***% error***	***L_1/L***	***L_1/L***	***% error***
				Actual	**ANN**		**Actual**	**ANN**	
24	0.933651	0.976141	0.979064	0.4	0.46422	**-13.83**	0.3125	0.31368	**-0.38**
25	0.912268	0.968767	0.973857	0.45	0.43949	**2.39**	0.3125	0.31363	**-0.36**
42	0.945748	0.861473	0.996031	0.5	0.55613	**-10.09**	0.46875	0.54979	**-17.29**
43	0.928886	0.829784	0.995012	0.55	0.56409	**-2.50**	0.46875	0.47352	**-1.02**
60	0.969514	0.783704	0.956052	0.60	0.71198	**-15.73**	0.625	0.62634	**-0.21**
61	0.957967	0.732205	0.947932	0.65	0.78834	**-17.55**	0.625	0.62731	**-0.37**
78	0.992363	0.837197	0.920514	0.70	0.74562	**-6.12**	0.78125	0.78647	**-0.67**
79	0.988453	0.776717	0.905112	0.75	0.79541	**-5.71**	0.78125	0.89982	**-15.18**
Predicted ANN results for U-shaped cracked cases									
Sr. No.	**f_{r1}**	**f_{r2}**	**f_{r3}**	***a/H***	***a/H***	***% error***	***L_1/L***	***L_1/L***	***% error***
				Actual	**ANN**		**Actual**	**ANN**	
24	0.939638	0.978116	0.980629	0.4	0.39789	**0.53**	0.3125	0.30495	**2.42**
25	0.919416	0.9711	0.975568	0.45	0.44714	**0.64**	0.3125	0.29721	**4.89**
42	0.951796	0.873472	0.996614	0.5	0.5026	**-0.52**	0.46875	0.4873	**-3.96**
43	0.935239	0.840919	0.995594	0.55	0.55417	**-0.76**	0.46875	0.48819	**-4.15**
60	0.972996	0.802134	0.958964	0.60	0.6038	**-0.63**	0.625	0.63822	**-2.12**
61	0.962304	0.750586	0.951573	0.65	0.65777	**-1.20**	0.625	0.63772	**-2.04**
78	0.993157	0.859726	0.928343	0.70	0.6921	**1.13**	0.78125	0.77927	**0.25**
79	0.989858	0.804913	0.912431	0.75	0.73425	**2.10**	0.78125	0.77935	**0.24**

Table 6. Comparison between Actual and predicted correlation model results of V-shaped and U-shaped cracked cases.

Predicted correlation model results for V-shaped cracked cases								
Sr. No.	**f_{r1}**	**f_{r2}**	***a/H***	***a/H***	***% error***	***L_1/L***	***L_1/L***	***% error***
			Actual	**Correlation model**		**Actual**	**Correlation model**	
24	0.933651	0.976141	0.4	0.3885	**2.88**	0.3125	0.2702	**13.54**
25	0.912268	0.968767	0.45	0.4052	**9.96**	0.3125	0.2862	**8.42**
42	0.945748	0.861473	0.5	0.5324	**-6.48**	0.46875	0.4969	**-6.01**
43	0.928886	0.829784	0.55	0.5852	**-6.40**	0.46875	0.5055	**-7.84**
60	0.969514	0.783704	0.60	0.6798	**-13.30**	0.625	0.7054	**-12.86**
61	0.957967	0.732205	0.65	0.8144	**-25.29**	0.625	0.7929	**-26.86**
78	0.992363	0.837197	0.70	0.7598	**-8.54**	0.78125	0.8493	**-8.71**
79	0.988453	0.776717	0.75	0.7141	**4.79**	0.78125	0.7993	**-2.31**
Predicted correlation model results for U-shaped cracked cases								
Sr. No.	**f_{r1}**	**f_{r2}**	***a/H***	***a/H***	***% error***	***L_1/L***	***L_1/L***	***% error***
			Actual	**Correlation model**		**Actual**	**Correlation model**	
24	0.939638	0.978116	0.4	0.3562	**10.95**	0.3125	0.2737	**12.42**
25	0.919416	0.9711	0.45	0.4038	**10.27**	0.3125	0.2711	**13.25**
42	0.951796	0.873472	0.5	0.4903	**1.94**	0.46875	0.4954	**-5.69**
43	0.935239	0.840919	0.55	0.5461	**0.71**	0.46875	0.5042	**-7.56**
60	0.972996	0.802134	0.60	0.6151	**-2.52**	0.625	0.6778	**-8.45**
61	0.962304	0.750586	0.65	0.7207	**-10.88**	0.625	0.7377	**-18.03**
78	0.993157	0.859726	0.70	0.5257	**24.90**	0.78125	0.6904	**11.63**
79	0.989858	0.804913	0.75	0.6935	**7.53**	0.78125	0.7997	**-2.36**

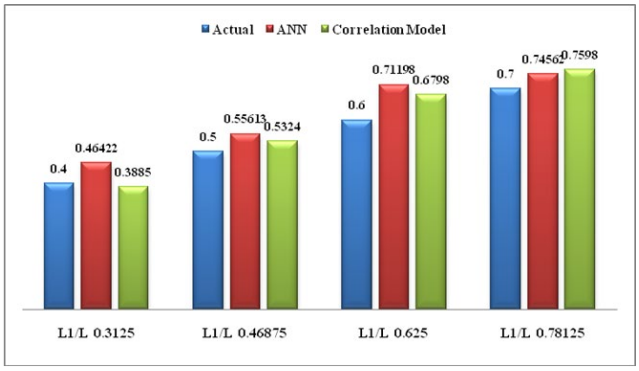

Figure 10. Predicted crack depth ratios using ANN and Correlation model at different crack location ratios.

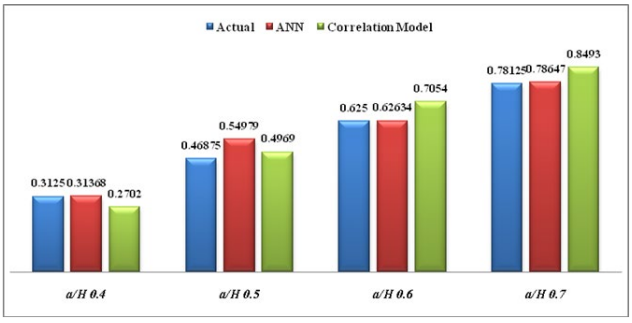

Figure 11. Predicted crack locations ratio using ANN and Correlation model at different crack depth ratio.

It is also apparent that, for the identical configurations, the natural frequency decrease of a U-shaped cracked beam compared to an un-cracked beam is considerably larger than that of a V-shaped cracked beam. As a result, it is clear that as the difference in natural frequency between the un-cracked and cracked beams grows; the ANN model can more accurately predict the crack characteristics. Similarly, when comparing the findings of Table 6, it is evident that the correlation model comparatively performed well in predicting the crack depths and positions in V-shaped cracked cases of beams. As a result, the correlation model can better predict the occurrence of V-shaped cracks than U-shaped cracks in beams for the same configurations.

8. CONCLUSIONS

The presence of crack changes the stiffness and vibration response of the beam. The crack development in a beam causes it to fail suddenly and without warning. Structural health monitoring is required to avoid hazards, damages, and breakdowns. In this research study, the natural frequencies of the un-cracked and cracked beams were evaluated using numerical method. Afterward, the correlation model

is developed for V-shaped and U-shaped cracked cases to predict the crack parameters in the beam. Furthermore, Machine learning approaches, i.e., artificial neural network (ANN), were utilized for the crack detection in beams. The following conclusions can be drawn from this research:

1. The beams' crack locations and depths can be accurately predicted using the correlation model, ANN, and the Discriminant Analysis Algorithm.
2. The correlation model predicts crack parameters more accurately in V-shaped cracked beams than U-shaped cracked beams for the same configurations.
3. According to the findings of this study, the ANN model is more accurate than other Machine Learning models at predicting the crack locations and crack depths in beams.
4. For the identical configurations, structural health monitoring utilizing a machine learning approach for U-shaped cracked cases is comparatively more successful than V-shaped cracked instances.

9. FUTURE SCOPE

A neural controller can be made and installed in structures using the ANN algorithm and can be programmed according to it, predicting the damages and providing prior warning and indication.

REFERENCES

[1] Vakil-Baghmisheh, M.T., Peimani, M., Sadeghi, M.H., & Ettefagh, M.M., *Crack detection in beam-like structures using genetic algorithms,* Applied soft computing, 8(2), 2008, pp. 1150–1160.

[2] Khatir, A., Tehami, M., Khatir, S., & Wahab, M.A., *Multiple damage detection and localization in beam-like and complex structures using co-ordinate modal assurance criterion combined with firefly and genetic algorithms,* Journal of Vibroengineering, 18(8), 2016, pp. 5063–5073.

[3] Sutar, M.K., Pattnaik, S., & Rana, J., *Neural Based Controller for Smart Detection of Crack in Cracked Cantilever Beam,* Materials Today: Proceedings, 2(4-5), 2015, pp. 2648–2653.

[4] Nasiri, S., Khosravani, M.R., & Weinberg, K., Fracture *mechanics and mechanical fault detection by artificial intelligence methods:* A review, Engineering Failure Analysis, 81, 2017, pp. 270–293.

[5] Teidj, S., Khamlichi, A., & Driouach, A., *Identification of beam cracks by solution of an inverse problem,* Procedia Technology, 22, 2016, pp. 86–93.

[6] Thatoi, D.N., Choudhury, S., Das, H.C., Jena, P.K., & Agrawal, G., CFBP Network–A Technique for Crack Detection, Procedia materials science, 6, 2014, pp. 10–17.

[7] Pan, D.G., Lei, S.S., & Wu, S.C., Two-*stage damage detection method using the artificial neural networks and genetic algorithms,* In International Conference on Information Computing and Applications, 2010, pp. 325–332.

[8] Orhan, S., Luy, M., Dirikolu, M.H., & Zorlu, G.M., The *effect of crack geometry on the non-destructive fault detection in a composite beam,* International Journal of Acoustics and Vibration, 21(3), 2016, pp. 271–273.

[9] ANSYS Release 12.1, ANSYS Inc.

[10] Khalkar, V., & Ramachandran, S., *The effect of crack geometry on non-destructive fault detection of EN 8 and EN 47 cracked cantilever beam,* Journal of Noise and Vibration Worldwide, 50, 2019, pp. 92–100.

[11] Khalkar, V., & Ramachandran, S., *The effect of crack geometry on stiffness of spring steel cantilever beam,* Journal of low frequency noise, vibration and active control, 37, 2018, pp. 762–774.

[12] Margaret, H.D., *Data Mining Introductory and Advanced Topics*, Pearson Education, 2008, India.

[13] Christianini, N., & Shawe-Taylor, J.C., *An Introduction to Support Vector Machines and Other Kernel-based Learning Methods*, Cambridge, U.K. Cambridge University, Press, 2000.

[14] Ian, H.W., Eibe, F, & Mark, A.H., *Data Mining*, 3rd Edition Morgan Kaufmann publisher, 2011

[15] Elaine, R., & Kevin, K, *Artificial Intelligence,* Third Edition, Tata McGraw-Hill Education Pvt. Ltd., 2008

[16] Fawcett, T., *An Introduction to ROC Analysis,* Pattern Recognition, 2006.

[17] Gillich, N., Tifisi, C., Sacarea, C., Rusu, C.V., Gillich, G., Praisach, Z., & Ardeljan, M., *Beam Damage Assessment Using Natural Frequency Shift and Machine Learning, Sensors,* 22, 2022, pp. 2–23.

[18] Tufisi, C., Gillich, N., Ardeljan, M., Paun, R.L., Rusu, V., & Gillich, G., *A Cost Function to Assess Cracks in Simply Supported Beams with Artificial Intelligence,* Romanian Journal of Acoustics and Vibration, 18(1), 2021, pp. 46–52.

[19] Tufisi, C., Rusu, C.V., Gillich, N., Pop, M.V., Hamat, C.O., Sacarea, C., & Gillich, N. (2022). *Determining the Severity of Open and Closed Cracks Using the Strain Energy Loss and the Hill-Climbing Method,* Applied Science, 12, 2022, pp. 2–18.

[20] Tufisi, C., Rusu, V., & Gillich, G., *Locating Transverse Cracks in Prismatic Beams Using Random Forest Method and the Frequency Drop,* Romanian Journal of Acoustics and Vibration, 18(2), 2021, pp. 119–125.

[21] Onchis, D.M., & Gillich, G., *Stable and explainable deep learning damage prediction for prismatic cantilever steel beam,* Computers in Industry, 125, 2021, pp. 1–8.

[22] Khalkar, V. Kumbhar, S.G., Hariharsakhtisudhan, P., Moshi, A.M.M., Jadhav, S.D., Kumbhar, N., Oak, P., & Joshi, P.S., *Some Studies on Verifying the Applicability of Free Vibration-based Modes Shapes Method to Rectangular Shaped Cracks in a Cantilever Beam,* U.Porto Journal of Engineering, 8 (2), 2022, pp. 82-94.

[23] Khalkar, V. Kumbhar, S.G., Logesh, K., Hariharsakhtisudhan, P., Jadhav, S.D., Danawade, B.A., Gharat, S.H., Jugulkar, L.M., Borade, J.G.., Experimental and numerical investigation of a cracked cantilever beam for damping loss factor to access its applicability in the crack detection*,* U.Porto Journal of Engineering, 8 (2), 2022, pp. 169-186.